symmetry

MDPI

Article

Symmetric Chaotic Behavior in 4D Variable-Order Fractional Systems Under Liouville–Caputo Operators

Mohamed Elbadri [1,*], Nidal E. Taha [2,*], Walid Hdidi [1], Hamdy M. Barakat [1] and Mohamed A. Abdoon [3]

1 Mathematics Department, College of Science, Jouf University, Sakaka 72388, Saudi Arabia
2 Department of Mathematics, College of Science, Qassim University, Buraidah 51452, Saudi Arabia
3 Department of Basic Sciences, Common First Year Deanship, King Saud University, P.O. Box 1142, Riyadh 12373, Saudi Arabia
* Correspondence: melbadri@ju.edu.sa (M.E); n.taha@qu.edu.sa (N.E.T.)

Abstract

In this paper, a novel four-dimensional variable-order fractional chaotic system is presented through the use of the Liouville–Caputo variable-order fractional derivative to represent the time-varying memory properties of nonlinear dynamical behaviors. Special attention will be paid to the chaotic behavior of the proposed system and their chaotic attractors depending on different memory effects. For calculation of the solutions of such systems, a numerical approach for the variable-order fractional systems is used, and three memory functions of the variable order are considered to investigate their effect on the behavior of the system. The obtained behavior will be analyzed by means of time responses, phase portraits, bifurcation diagrams, the spectrum of the Lyapunov exponents, and the Kaplan–Yorke fractal dimension. From the numerical simulations, it is shown that different fractional orders lead to completely different dynamical regimes and the appearance of symmetric chaotic attractors with different geometrical and topological structures while the physical parameters of the system are kept the same. These results highlight the important role of time-varying memory in controlling and generating chaotic structures in fractional-order nonlinear systems.

Keywords: fractional variable-order; Chaos; bifurcation; Lyapunov exponents; numerical methods

MSC: 34A08; 65L20; 37G35

1. Introduction

Fractional systems are modeled because nonlocal interactions and historical memory have been incorporated into the nature of differential operators [1–4]. Recently, variable-order fractional calculus has gained much attention in the analysis of nonlinear dynamical systems and chaotic phenomena, owing to its ability to capture time-dependent memory effects. In contrast to the constant-order models, the use of the variable-order models introduces another parameter that allows for the realistic modeling of dynamical systems with varying memory properties [5,6].

Because of its capability in the modeling of different natural phenomena, such as anomalous diffusion and hereditary phenomena, among others, fractional calculus has been considered a robust tool for modeling dynamical systems behavior [4,7,8]. Though constant-order fractional models have been found useful in modeling stable hereditary behavior, they cannot model the behavior of heterogeneous systems whose memory changes

check for updates

Academic Editor: Calogero Vetro

Received: 12 August 2026
Revised: 5 September 2026
Accepted: 8 September 2026
Published: 11 September 2026

over time [9,10]. The great versatility provided by variable-order fractional derivatives is the reason why there has been great interest in them over the past years in studying nonstationary and heterogeneous systems. These derivatives have proved to be very useful in modeling complex dynamics associated with continuously varying internal structure, variable diffusivity, and time-dependent physical properties. VOFDs can be found in several fields such as viscoelasticity, control theory, bioengineering, signal processing, heat transfer, and anomalous transport processes [11,12].

Variable-order fractional (VOF) calculus is a strong and versatile tool for the mathematical modeling of dynamic processes that have time-dependent properties. The variable order approach makes it possible for the order of derivative to depend on time, space, or the state of the process under consideration, thus enabling the description of the evolution of the memory and hereditary properties more precisely than fixed-order derivatives do. Variable-order models can represent complex dynamic processes that have changing characteristics as time changes, thereby providing a better approximation to reality [13–15].

Apart from their applicability, variable-order fractional models have recently gained popularity in the theoretical study of nonlinear dynamical systems. The ability of such models to provide enhanced insight into the dynamical aspects of the system, such as stability transition, bifurcation, pattern formation, and chaos, among others, makes the variable order fractional calculus a useful mathematical method for studying the properties of fractional differential equations [16–18].

The recent developments in the field of fractional calculus have highlighted the increasing importance of fractional-order and variable-order fractional models in characterizing and studying the behavior of purpose systems. The use of these mathematical methods has proved to be especially useful for modeling systems possessing properties such as nonlocal interactions, hereditary behavior, and time-dependent memory that cannot be accounted for using classical integer-order methods. Therefore, the application of fractional and variable-order models has been gaining more and more relevance for the study of the dynamics of various complex phenomena [19].

Table 1 shows the differences between the presented framework and the relevant literature. Though the former research has analyzed some aspects of chaotic systems with fractional order (FO) and variable order (VOF), no framework has been suggested for analyzing such systems with respect to variable order fractional modeling, chaos analysis (CH), bifurcation analysis (BF), calculation of Lyapunov exponents (LES), and time series analysis (TS). The present framework covers all the above aspects in one package. Thus, the presented work is complete.

The increase in the use of these mathematical models is related to the increased accuracy of representing dynamic processes, in which the properties change over time. Specifically, the adaptability of the variable-order approach makes it possible to represent the changes in the process being studied, its memory properties, and external factors influencing it.

Moreover, theoretical and computational advancements have greatly broadened the horizons of fractional and variable-order calculus. Much success has been made in the area of building effective numerical schemes, creating computational methods for arbitrary variable-order derivatives, and designing robust analytical approaches for solving fractional differential equations. As a result, more complex and sophisticated models have become feasible to study.

Table 1. Comparison of representative studies and the proposed framework.

References	VOF	FO	CH	BF	LES	TS
[20]	×	✓	✓	×	×	×
[21]	×	✓	✓	×	×	×
[22]	×	✓	✓	×	✓	✓
[23]	✓	✓	✓	×	✓	✓
[24]	✓	✓	✓	✓	✓	✓
[25]	✓	✓	✓	✓	✓	✓
This work	✓	✓	✓	✓	✓	✓

Simultaneously, modern control theory has widely adopted fractional and variable-order approaches to develop new classes of controllers specifically designed for nonlinear and uncertain dynamic systems. Due to their potential to describe memory-related effects and complicated interactions within the system, the performance of such areas as system identification, adaptive control, optimization, signal processing, and fault diagnosis was greatly enhanced. Therefore, fractional and variable-order calculus continue to evolve as very effective mathematical apparatuses that provide new viewpoints and solutions to modern scientific problems [26–28].

The novelty of this article lies in extending a 4D chaotic system to a variable-order fractional system via the Liouville–Caputo (LC) operator for the efficient representation of time-varying memory coupling in monotonically increasing, periodic, and decaying regimes. This variable-order structure leads to the formation of uniquely structured chaotic attractors in the form of butterflies, multiple-layer ribbons, and diamond-ring shapes. The chaotic structure is supported with reliable bifurcation analysis and Lyapunov spectra analysis, which possesses one positive Lyapunov exponent and exceptionally high Kaplan–Yorke fractal dimension.

Figure 1 shows the complete workflow of the current study. In this way, after designing the fractional order models of constant and variable orders, the solutions are numerically obtained by applying the Newton polynomial interpolation. The theoretical study, which includes equilibrium, stability, and dissipativity analysis, is followed by the dynamical study using phase portraits, time series, Lyapunov exponents, and bifurcation diagrams.

The main contributions of this research work are listed below:

- We have been successful in extending the concept of the 4D chaotic system from a fixed order to a variable order with the help of the LC operator.
- They consist of an everlasting butterfly-type inner orbit shell with monotonically increasing property, a multi-layered ribbon type showing track-splitting phenomenon with periodic variation, and the diamond-ring type having an infinity symbol (∞) inside it, which shows asymptotic decay.
- An effective numerical method is employed in order to effectively capture the coupling of memory-dependent terms over three different operating regions (monotonic, periodic, and decay).
- According to the Lyapunov spectrum calculation, the occurrence of the chaos involving one positive LE is proved. As per comparison, it can be clearly seen that the proposed system possesses a maximum fractal dimension value ($D_{KY} \approx 3.0009$) which outperforms several other integer-order and fractional-order chaotic systems available in the recent literature.
- The concordance of the bifurcation diagram with the Lyapunov exponent spectrum indicates the rich dynamical behavior of the proposed system.

The novelty lies not in the formal substitution of the constant value of the fractional-order parameter α by a time-dependent variable $\alpha(t)$, but in the symmetric investigation of how monotonically increasing, periodic, and decaying memory functions reshape dynamics of the same nonlinear system with fixed physical parameters.

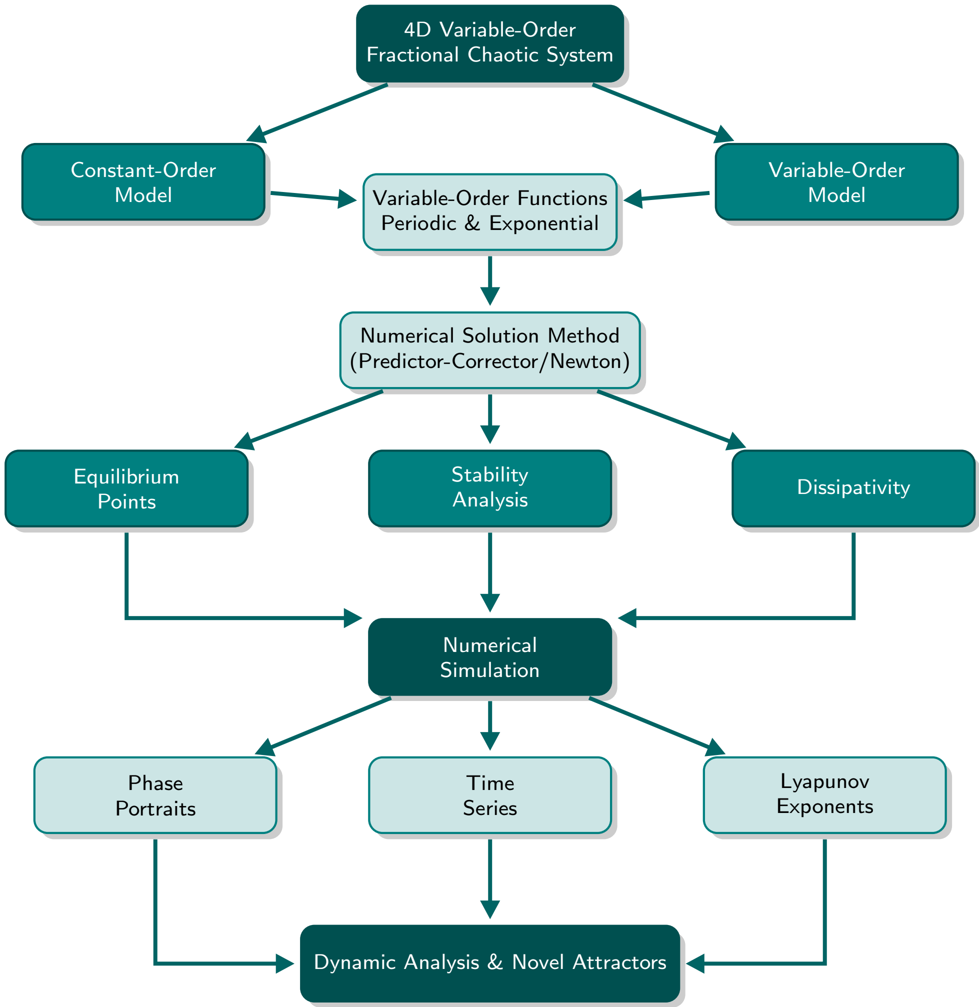

Figure 1. Professional workflow diagram of the variable-order fractional system analysis. The color scheme uses a monochromatic teal palette to distinguish between system initialization (dark teal), mathematical derivation (medium teal), and computational analysis (pale teal/white).

2. System Definition and Analysis

2.1. 4D Fractional Chaotic System

The fractional-order form of the proposed 4-dimensional chaotic system [29] is expressed as follows:

$$\begin{aligned} D_t^{\alpha} u_1 &= u_2, \\ D_t^{\alpha} u_2 &= -u_3 u_2 - u_1 - a_1 u_4, \\ D_t^{\alpha} u_3 &= a_2 u_2^4 - a_3 |u_2| - a_5, \\ D_t^{\alpha} u_4 &= -a_4 u_4 + u_2 u_3. \end{aligned} \tag{1}$$

where D_t^{α} denotes the fractional derivative of constant order α. The initial condition vector and parameter values are chosen as $(u_1, u_2, u_3, u_4) = (0.2, 0.3, 0.1, 0.5)$ and $a_1 = 0.5$, $a_2 = 0.9$, $a_3 = 1.5$, $a_4 = 5.5$, $a_5 = 1.6$, respectively. The parameter values and initial conditions were selected based on numerical simulations and bifurcation analyses to ensure the system exhibits robust chaotic behavior. These choices reliably reproduce the characteristic strange attractors of the fractional-order system.

2.2. 4D Variable-Order Fractional Chaotic System

To incorporate an evolving memory mechanism, the constant fractional order is replaced by time-dependent orders α, yielding the following new variable-order chaotic system:

$$\begin{aligned}
{}_{0}^{LC}\mathbb{D}_{t}^{\alpha(t)} u_1 &= u_2, \\
{}_{0}^{LC}\mathbb{D}_{t}^{\alpha(t)} u_2 &= -u_3 u_2 - u_1 - a_1 u_4, \\
{}_{0}^{LC}\mathbb{D}_{t}^{\alpha(t)} u_3 &= a_2 u_2^4 - a_3 |u_2| - a_5, \\
{}_{0}^{LC}\mathbb{D}_{t}^{\alpha(t)} u_4 &= -a_4 u_4 + u_2 u_3,
\end{aligned} \tag{2}$$

where ${}_{0}^{LC}\mathbb{D}_{t}^{\alpha(t)}$ denotes e Liouville–Caputo (LC) fractional VOF, , with $0 < \alpha(t) < 1$.

Equilibrium Points and Stability Analysis

To determine the equilibrium points of the system, the following algebraic system must be solved:

$$u_2 = 0, \tag{3a}$$

$$-u_3 u_2 - u_1 - a_1 u_4 = 0, \tag{3b}$$

$$a_2 u_2^4 - a_3 |u_2| - a_5 = 0, \tag{3c}$$

$$-a_4 u_4 + u_2 u_3 = 0. \tag{3d}$$

From Equation (3a), the condition $u_2 = 0$ is obtained. Upon substitution of $u_2 = 0$ into Equation (3c), the relation $-a_5 = 0$ is derived. Although Equation (3c), considered in isolation, $a_2 u_2^4 - a_3 |u_2| - a_5 = 0$, admits real nonzero roots, none of these roots satisfies Equation (3a), which rigorously imposes $u_2 = 0$ as a necessary condition for any equilibrium. Hence, no branch with $u_2 \neq 0$ exists to be examined. This leads to a contradiction because a_5 is a positive constant. It is therefore concluded that the proposed system admits no equilibrium points. Consequently, conventional local stability analysis based on equilibrium point linearization and the Matignon criterion cannot be performed. Hence, any attractor the system exhibits is necessarily a hidden attractor, since its basin of attraction cannot intersect any neighborhood of an equilibrium point.

3. Computational Numerical Scheme

In this part, numerical schemes used to solve the proposed fractional-order dynamic model with FO and VFO are given. In this context, the same prediction–correction approach is used for both schemes where the variable-order scheme extends the constant-order one by using a time-varying fractional order.

3.1. Preliminaries

Definition 1 ([30])**.** *The LC-FO of* α $(0 < \alpha < 1)$ *is defined as*

$$^{LC}\mathcal{D}_t^{\alpha} y(t) = \frac{1}{\Gamma(1-\alpha)} \int_0^t (t-\tau)^{-\alpha} \frac{d}{d\tau} y(\tau)\, d\tau, \qquad 0 < \alpha < 1. \tag{4}$$

Definition 2 ([31])**.** *The LC-VFO is defined by*

$$^{LCV}\mathcal{D}_t^{\alpha(t)} y(t) = \frac{1}{\Gamma(1-\alpha(t))} \int_0^t (t-\tau)^{-\alpha(t)} y'(\tau)\, d\tau, \qquad 0 < \alpha(t) < 1. \tag{5}$$

The constant order Liouville–Caputo operator considers the same memory effect in the entire period of the dynamics. On the other hand, the variable order model employs a time-varying order of differentiation; thus, the memory strength is allowed to change continuously during the simulation process. This approach makes the variable order operator very convenient for modeling nonlinear systems with time-varying hereditary properties.

3.2. Variable-Order Numerical Approximation

For the effective numerical simulation of the proposed nonlinear fractional system, the predictor–corrector method using the Liouville–Caputo fractional derivative is employed. Numerical realization is based on the methodology introduced in [32,33]. The obtained approximation takes the form

$$\mathbf{U}_{n+1} = \mathbf{U}_0 + \frac{1}{\Gamma(\alpha(t_n))} \sum_{j=0}^{n} \frac{h^{\alpha(t_n)}}{\alpha(t_n)[\alpha(t_n)+1]} \left[G(t_j, \mathbf{U}_j)\, R_{n,j} - G(t_{j-1}, \mathbf{U}_{j-1})\, T_{n,j} \right]. \quad (6)$$

where

$$\begin{aligned} R_{n,j} &= (n+1-j)^{\alpha(t_n)}(n-j+2+\alpha(t_n)) - (n-j)^{\alpha(t_n)}(n-j+2+2\alpha(t_n)), \\ T_{n,j} &= (n+1-j)^{\alpha(t_n)+1} - (n-j)^{\alpha(t_n)}(n-j+1+\alpha(t_n)). \end{aligned} \quad (7)$$

Here, $G_i(t, \mathbf{U})$ denotes the nonlinear function corresponding to the ith state equation of the proposed fractional-order dynamical system.

For the proposed four-dimensional nonlinear system, the vector-valued nonlinear function is defined by

$$\begin{aligned} G_1 &= u_2, \\ G_2 &= -u_3 u_2 - u_1 - a_1 u_4, \\ G_3 &= a_2 u_2^4 - a_3 |u_2| - a_5, \\ G_4 &= -a_4 u_4 + u_2 u_3. \end{aligned} \quad (8)$$

Accordingly, the numerical implementation evaluates the nonlinear vector $\mathbf{G}(t, \mathbf{U})$ at each integration step and substitutes the computed values into the predictor–corrector formulations given in (6). This recursive procedure generates the numerical trajectories of the proposed fractional-order systems.

4. Dynamical Analysis

In the next section, the chaotic dynamics of System 2 is described by various approaches [34,35]. The chaotic dynamics is studied by phase space representation, time series, Lyapunov exponents and attractors. These techniques demonstrate chaos, qualitative change in the behavior of the system and unpredictability of the system dynamics. The simulations are extended to larger intervals of time (up to $t = 100$) to allow for the complete decay of initial transients and the system to settle down in its true asymptotic regime. Thus, the phase portraits correspond to the fully developed chaotic attractors, not the short-term transient fluctuations.

4.1. Multi-Case System Analysis

The system described in Equation (2) was numerically solved over the time interval $[0, 100]$. The resulting phase portraits are shown under two distinct scenarios.

Case 1: In this case, the order $\alpha(t)$ is taken as follows: $\alpha(t) = 0.98 + 0.01\tanh(t)$. The above form of the function is chosen to describe the process of smooth and monotonous change of the fractional order.

Case 2: For this case, the order function is specified as $\alpha(t) = 0.984 + 0.006\cos(\pi t/10)$. This study uses this example to analyze the system's sensitivity to oscillations of the derivative order.
Case 3: For this case, the definition of the order is given by $\alpha(t) = 0.98 + 0.01e^{-t}$. This type of setup is chosen to study the effect of a decaying variable order with exponential order approaching a constant value that eventually reaches a fractional order state.

In order to obtain the unique time-dependent nature of memory in the system, we consider three different variable-order models for $\alpha(t)$. The first one is the monotonic increase model Case 1 which represents an accumulating effect of memory resulting in the expansion of phase space structures, the second one is the periodic model Case 2 which introduces oscillatory effects leading to ring-like attractors, and the third one is the exponential decrease model Case 3.

Simulation Steps

1. Set the parameters and initial conditions from Table 2.
2. Select the time grid $t_n = nh$ with step size $h = 0.01$.
3. Choose one of the three variable-fractional-order laws from Table3.
4. At each time step, evaluate the nonlinear vector terms g_1, g_2, g_3, g_4.
5. Apply the LC fractional numerical scheme using the two-step Newton's interpolation polynomial method to update the state trajectories u_1, u_2, u_3, u_4.
6. Repeat the calculations across the three separate memory regimes and evaluate the resulting chaotic trajectories.

Table 2. Parameters, initial conditions, and variable-order settings for simulations of System 2.

Category	Parameters/Settings
Variable-fractional orders	$\alpha(t) = 0.98 + 0.01\tanh(t)$ (Case 1) $\alpha(t) = 0.984 + 0.006\cos\left(\frac{\pi t}{10}\right)$ (Case 2) $\alpha(t) = 0.98 + 0.01e^{-t}$ (Case 3)
System parameters	$a_1 = 0.5$, $a_2 = 0.9$, $a_3 = 1.5$, $a_4 = 5.5$, $a_5 = 1.6$
Step size Initial conditions	$h = 0.01$ $(u_1(0), u_2(0), u_3(0), u_4(0)) = (0.2, 0.3, 0.1, 0.5)$

Table 3. Cases of the fractional variable order

Case	Formula	$t = 100$	$t = 200$	Range
1	$0.98 + 0.01\tanh(t)$	0.99	0.99	$[0.98, 0.99]$
2	$0.984 + 0.006\cos\left(\frac{\pi t}{10}\right)$	0.99	0.99	$[0.978, 0.99]$
3	$0.98 + 0.01e^{-t}$	0.98	0.98	$(0.98, 0.99]$

4.2. Bifurcation and Lyapunov Exponent

The bifurcation diagram and the corresponding Lyapunov exponent (LE) spectra of the proposed system in three different scenarios are given in Figures 2–4. As can be seen, there is a topological change in the dynamics of the system from chaotic dynamics to stable periodic orbits for larger parameter values. Such changes are strictly tested using the LE spectra, i.e., the presence of chaos is proven by the positivity of the largest Lyapunov exponent ($LE_1 > 0$), and otherwise, it is equal to zero or less than zero ($LE_1 \leq 0$).

In all three cases where the variable order exists, a favorable chaotic state is observed with $LE_1 > 0$ within the parameter range of $a_3 \in [0, \approx 2.4]$, while Case 2 exhibits periodic windows that appear amid its chaotic windows. However, as the value of the parameter

a_3 exceeds approximately 2.4–2.6, the system moves to the periodic orbit through reverse period doubling.

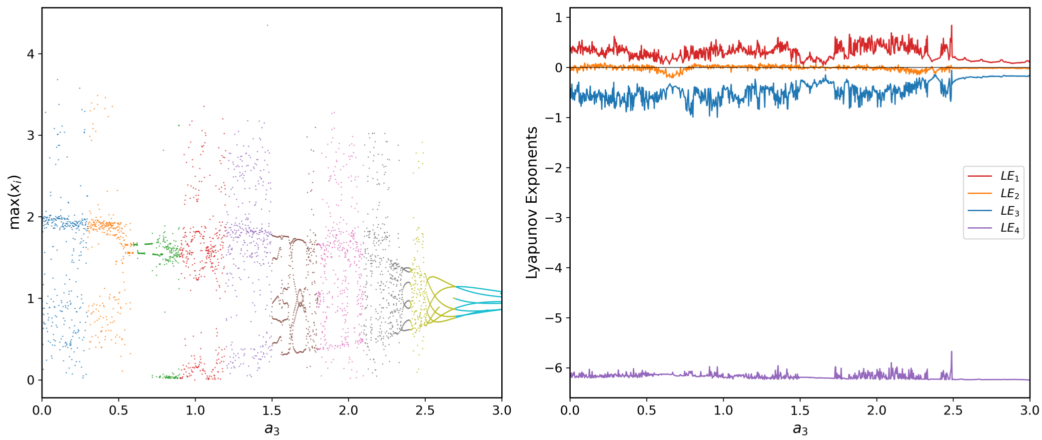

Figure 2. Bifurcation diagram and Lyapunov exponent spectrum for Case 1.

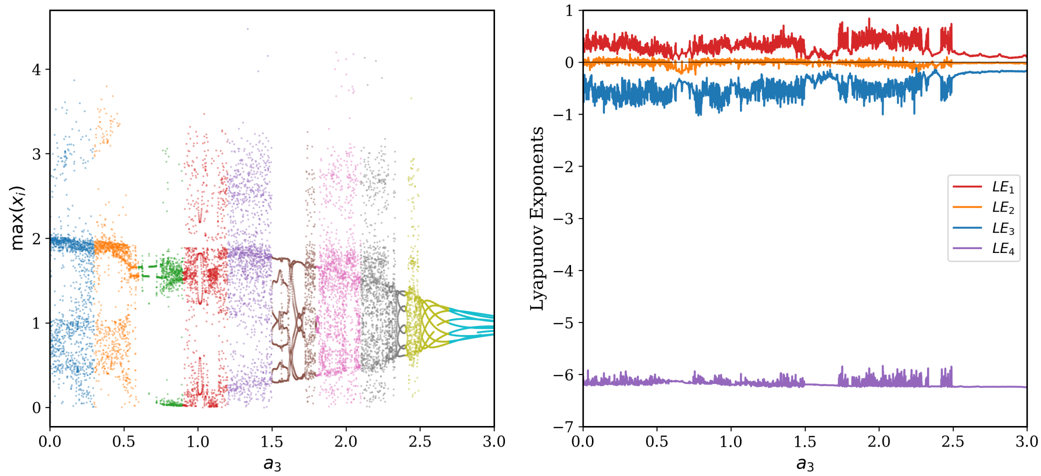

Figure 3. Bifurcation diagram and Lyapunov exponent spectrum for Case 2.

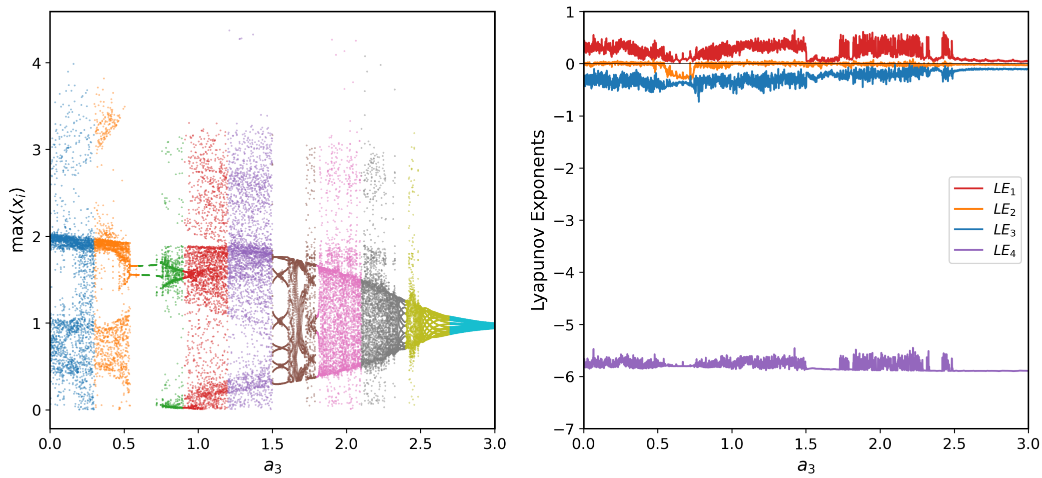

Figure 4. Bifurcation diagram and Lyapunov exponent spectrum for Case 3.

4.3. Lyapunov Exponents

In this part, the convergence of the Lyapunov exponent spectrum in real time for Cases 1, 2, and 3 is illustrated in Figures 5–7, correspondingly. In spite of initial transient fluctuations during the first time interval ($t < 20$ s), the trajectories of all exponents tend toward stable asymptotic values. Convergence of at least one positive exponent over long periods of time is proof of the existence of chaotic behavior in the fractional-order system (2).

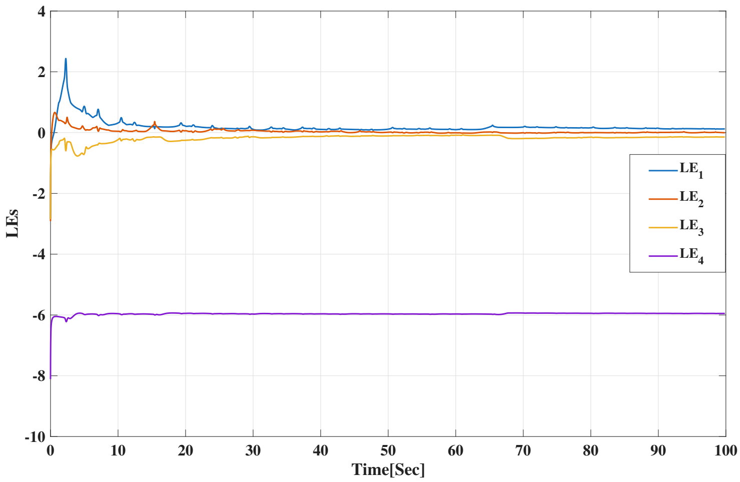

Figure 5. Lyapunov exponent spectrum over time for Case 1.

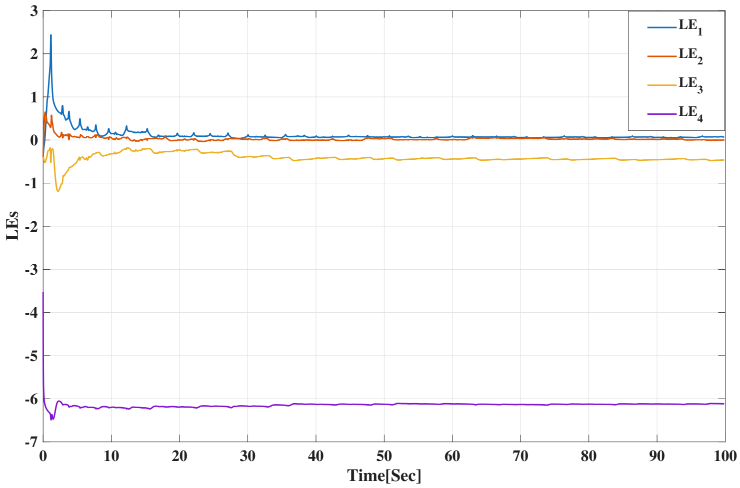

Figure 6. Lyapunov exponent spectrum over time for Case 2.

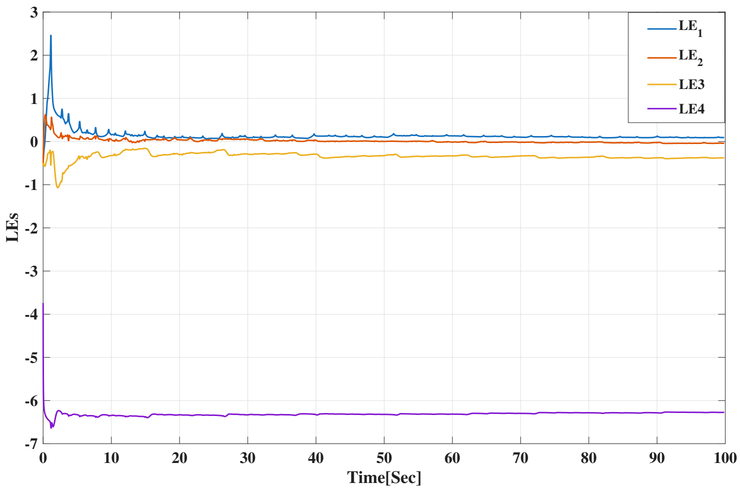

Figure 7. Lyapunov exponent spectrum over time for Case 3.

The sensitivity of the VOFC was verified using the calculation of the asymptotic Lyapunov exponents and Kaplan–Yorke dimensions (D_{KY}) at two different integration step sizes, namely $h = 0.01$ and $h = 0.005$. Based on Table 4, it is clear that the system exhibits chaotic and chaotic behavior regardless of the selected time step.

(D_{KY}) is defined as

$$D_{\mathrm{KY}} = j + \frac{\sum_{i=1}^{j} \lambda_i}{|\lambda_{j+1}|}, \tag{9}$$

where j is the largest integer for which $\sum_{i=1}^{j} \lambda_i > 0$.

More precisely, Cases 1 and 3 show chaotic behavior at a stable state, which features one positive exponent ($\mathrm{LE}_1 > 0$) for both values of the step size, fixing the fractal dimension at approximately $D_{\mathrm{KY}} \approx 2.45$. In Case 2, reducing the value of the step size from $h = 0.01$ to $h = 0.005$ changes the value of the second exponent from a slightly negative value to a positive value ($\mathrm{LE}_2 = 0.0120$), indicating a high sensitivity to periodic variation, leading to chaos.

Table 4. The Lyapunov exponents and Kaplan–Yorke dimension (D_{KY}) across different cases.

Cases	h	LE_1	LE_2	LE_3	LE_4	D_{KY}
Case 1	0.01	0.0719	0.0000	−0.1590	−5.9378	2.4523
	0.005	0.0809	0.0000	−0.0948	−5.9178	2.8534
Case 2	0.01	0.0649	0.0000	−0.1092	−6.1224	2.5941
	0.005	0.0818	0.0000	−0.0763	−6.1048	3.0009
Case 3	0.01	0.0785	0.0000	−0.0766	−6.2825	3.0003
	0.005	0.0665	0.0000	−0.0608	−6.2826	3.0009

As shown in Table 4, all cases exhibit a single positive Lyapunov exponent ($\mathrm{LE}_1 > 0$) alongside a zero exponent ($\mathrm{LE}_2 = 0$), confirming standard chaotic dynamics rather than hyperchaos. The Kaplan–Yorke dimension (D_{KY}) remains fractional across all variations of step size h, further verifying the presence of strange attractors.

The D_{KY} to quantify the complexity and fractal behavior of the chaotic attractors is based on the Lyapunov exponent (LE) spectra. The dimension is a quantified measure of the strangeness of the system and hence helps to compare the level of chaos in different systems. The following table summarizes a comparison of the Kaplan–Yorke fractal dimension, the number of positive LEs, and the dynamics of different four-dimensional systems, including the suggested system.

The results suggest that the number of positive Lyapunov exponents—between one and two—essentially controls the dynamical behavior of each system. Specifically, systems featuring a single positive LE, such as [36–39], exhibit standard chaotic dynamics. Conversely, systems with one positive LE, including [40] and the three cases proposed in this study, fall into the chaotic category.

The D_{KY} from the point of view of complexity theory acts as a numerical criterion for estimating the geometric complexity of the attractor. The literature reviewed shows that the smallest Kaplan–Yorke dimension in [38] is $D_{\mathrm{KY}} = 2.0767$, whereas the maximum complexity in the literature considered separately is [39] with $D_{\mathrm{KY}} = 2.825$.

More importantly, the proposed system exhibits excellent results in terms of complexity measures since it is better than all literature-based systems with respect to these parameters. For Case 1, the KY dimension is determined as 2.8534, which means that the complexity degree is relatively high. What is more important, for Case 2 and Case 3, the KY dimension is significantly increased to 3.0009. The higher value proves the fact that the chaotic attractors' structure is highly complex. Finally, all three cases of the proposed system exhibit strong chaotic dynamics due to one positive Lyapunov exponent.

https://doi.org/10.3390/sym18091525

The comparative study of the Lyapunov exponent spectra and Kaplan–Yorke dimensions (D_{KY}) in Table 4 reveals that the three variable-order memory profiles with hyperbolic tangent (Case 1), periodic cosine (Case 2), and exponential decay (Case 3) all have positive maximal Lyapunov exponents ($LE_1 > 0$), which confirms the existence of chaos, while the different memory profiles influence the expansion rates and the fractal dimensions. In particular, Case 3 shows the largest initial positive exponent ($LE_1 = 0.0785$ at $h = 0.01$), while Case 2 displays an increased sensitivity to step-size refinement, which results in an increase in the Kaplan–Yorke dimension ($D_{KY} = 3.0009$ at $h = 0.005$). These quantitative trends suggest that the variations in the historical memory profile influence mostly the geometric complexity and the local tightness of the attractors, rather than switching the underlying chaotic regime.

A comparison between the computed values of the Kaplan–Yorke dimensions and those for some other four-dimensional chaotic systems, presented in Table 5, reveals the higher values of dimensions for the proposed cases of variable order (up to 3.0009). Despite the fact that this quantity stresses the increased complexity of the geometric configuration and folding of the phase space for the selected memory functions, it is important to remember that the Kaplan–Yorke dimension is a particular criterion of the attractor complexity and not a general criterion of system superiority.

Table 5. Kaplan–Yorke fractal dimension of eight chaotic systems.

System	Dimension	Positive LEs	Type	D_{KY}
[36]	4D	1	Chaotic	2.2326
[37]	4D	1	Chaotic	2.5790
[38]	4D	1	Chaotic	2.0767
[40]	4D	2	Hyperchaotic	2.7995
[39]	4D	1	Chaotic	2.825
This study (Case 1)	4D	**1**	Chaotic	2.8534
This study (Case 2)	4D	**1**	Chaotic	3.0009
This study (Case 3)	4D	**1**	Chaotic	3.0009

4.4. *Chaos Analysis*

The numerical simulations for determining the structural development of the system were done on two different time scales ($t = 100$ and $t = 200$). The 2D and 3D phase diagrams obtained reveal highly complicated topological structures which indicate the emergence of new chaotic states arising due to the variable-order fractional dynamics.

Figures 8 and 9 showcase the phase diagrams of the 4D chaotic system. As can be observed in Figure 8, the traditional integer-order approach with $\alpha = 1$ yields very dense and continuous chaotic attractors. However, the application of a fractional order in the system ($\alpha = 0.99$), as shown in Figure 9, completely changes the topology of the chaotic system due to the effect of the memory in the system.

- **Case 1: Monotonic Smooth Transition (Figures 10 and 11)**
  The orbits of the phase portrait for $\alpha(t) = 0.98 + 0.01\tanh(t)$ show that there is a butterfly-like attractor with an inner orbit shell. From the orbit distribution at $t = 100$ (Figure 10) to the orbit distribution at $t = 200$ (Figure 11), the orbit density fills out seamlessly without altering the geometric boundary. This stable evolution confirms a clean, self-sustaining novel chaotic state during smooth order variation.
- **Case 2: Periodic Fluctuations (Figures 12 and 13)**
  The attractor is forced by $\alpha(t) = 0.984 + 0.006\cos(\pi t/10)$, and the attractor morphs into a novel, multi-layered ribbon structure. The explicit comparison between Figure 12 and Figure 13 shows that the internal track-splitting is varying continuously

under the periodic variation, but the globally bounded chaotic envelope is perfectly robust.

- **Case 3: Asymptotic Exponential Decay (Figures 14 and 15)**
  Under the decaying functional order $\alpha(t) = 0.98 + 0.01e^{-t}$, the system stabilizes into an entirely new geometric archetype: a sharp, diamond-ring-shaped outer loop enclosing an infinity-symbol (∞) core. The exceptional overlap between $t = 100$ (Figure 14) and $t = 200$ (Figure 15) shows that once the transient exponential term decays, the system locks firmly into a stationary, novel fractional chaotic state.

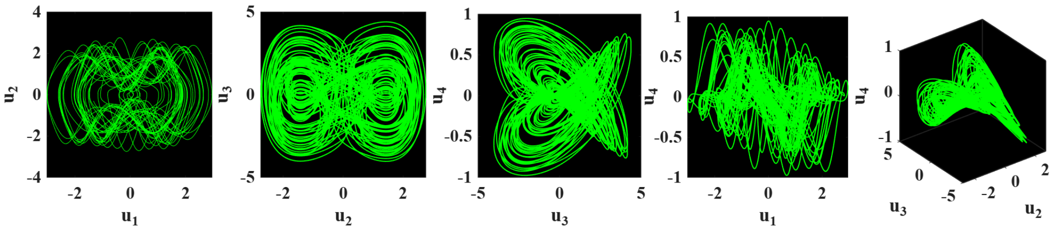

Figure 8. Chaotic phase portraits of the system for the classical-order case ($\alpha = 1$).

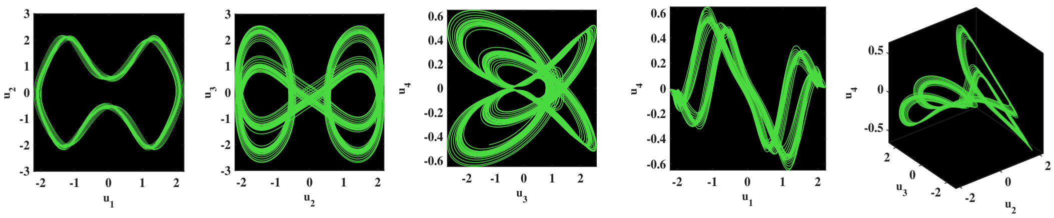

Figure 9. Chaotic phase portraits of the system for the fractional-order case ($\alpha = 0.99$).

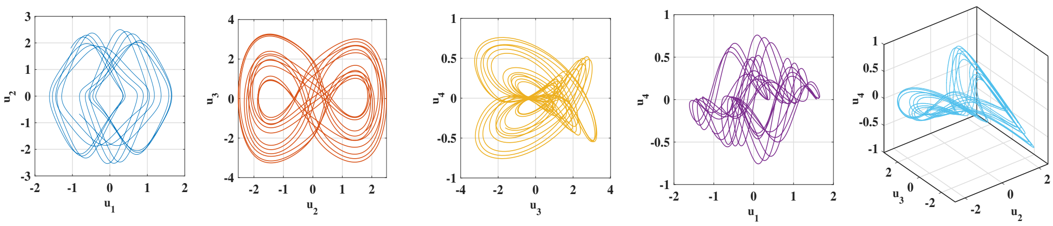

Figure 10. Chaotic phase portraits of the system for Case 1 at $t = 100$.

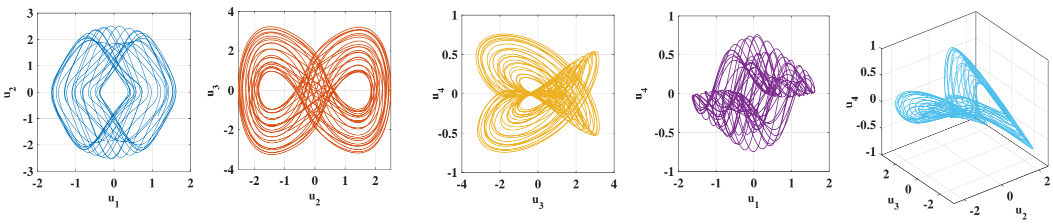

Figure 11. Chaotic dynamics depicted via phase portraits for Case 1 at $t = 200$.

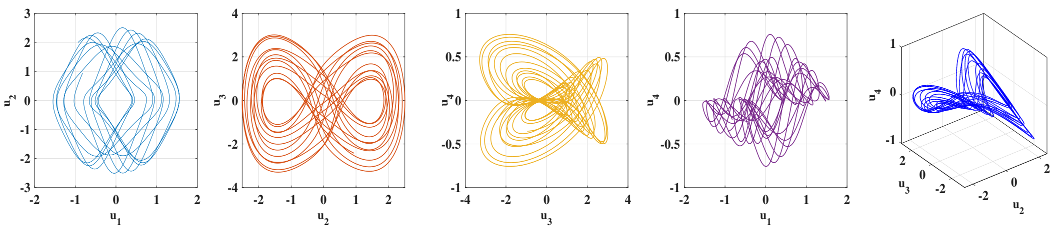

Figure 12. Chaotic dynamics depicted via phase portraits for Case 2 at $t = 100$.

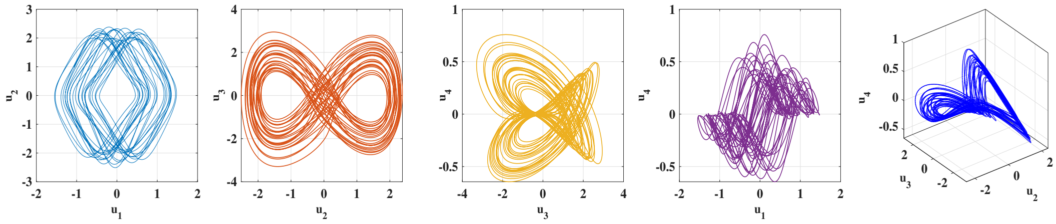

Figure 13. Chaotic dynamics depicted via phase portraits for Case 2 at $t = 200$.

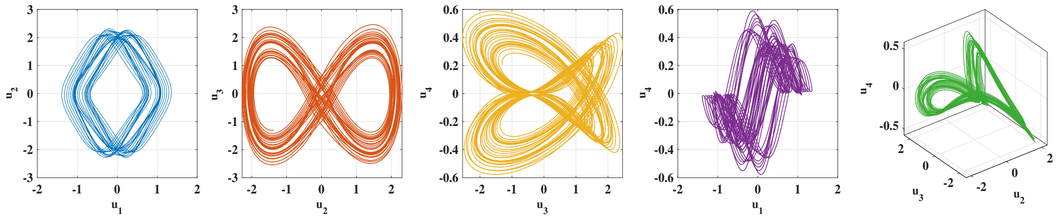

Figure 14. Chaotic phase portraits of the system for Case 3 at $t = 100$.

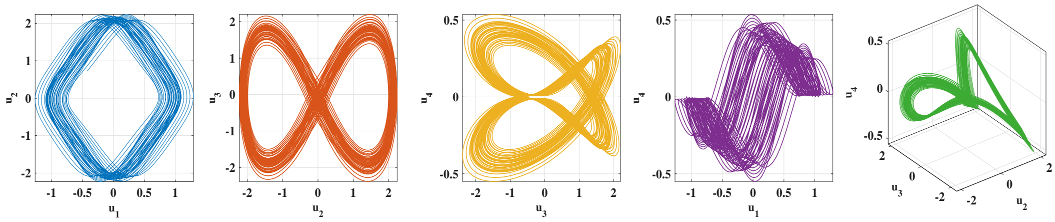

Figure 15. Chaotic phase portraits of the system for Case 3 at $t = 200$.

4.5. Time Series Analysis

In addition to the phase portraits, we study the short-term ($t \in [0, 100]$) and long-term ($t \in [100, 200]$) temporal evolutions of the state variables (u_1, u_2, u_3, u_4). The time series plots show very non-periodic, erratic waveforms confirming continuous chaotic oscillations for all the configurations.

- **Case 1 (Figures 16 and 17)**
  For the parameter change function $\alpha(t) = 0.98 + 0.01\tanh(t)$, where the transition from the transient states at the beginning (Figure 16) to a dense, continuous chaotic wave train occurs in the $[100, 200]$ range (Figure 17). The fact that no amplitude decay or periodicity is observed confirms this.
- **Case 2 (Figures 18 and 19)**
  The dynamics of the system when driven through the oscillating function$\alpha(t) = 0.984 + 0.006\cos(\pi t/10)$ produces a time series with clear variation in the envelopes corresponding to the slow periodic drive (Figure 18). On a larger time scale (Figure 19), these envelopes produce high-frequency bursts with great randomness.
- **Case 3 (Figures 20 and 21)**
  In the case of the exponentially decaying profile of memory described by the function $\alpha(t) = 0.98 + 0.01e^{-t}$, one can observe the amplitude fluctuations only for $t < 50$ (Figure 20). When the variable order of the equation comes to its steady state in the longtime regime (Figure 21), the waveforms become a structurally uniform but completely chaotic oscillation.

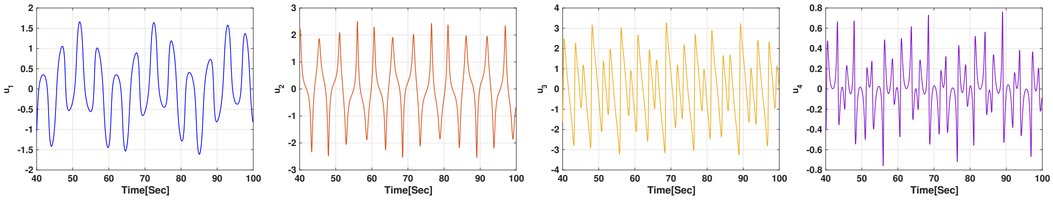

Figure 16. Time-series evolution of the states for Case 1 at $t = 100$.

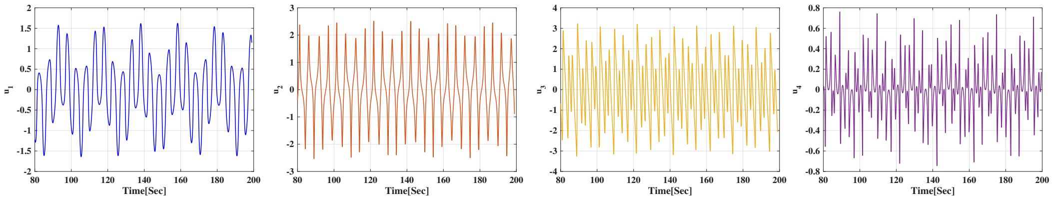

Figure 17. Time-series evolution of the states for Case 1 at $t = 200$.

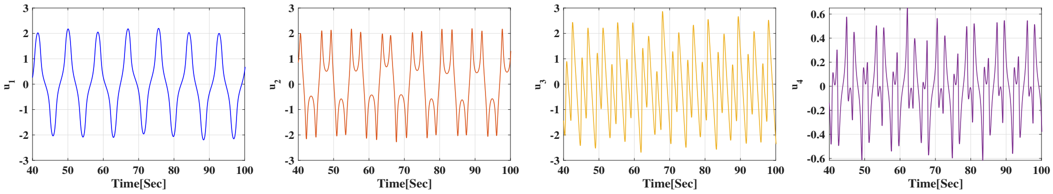

Figure 18. Time-series evolution of the states for Case 2 at $t = 100$.

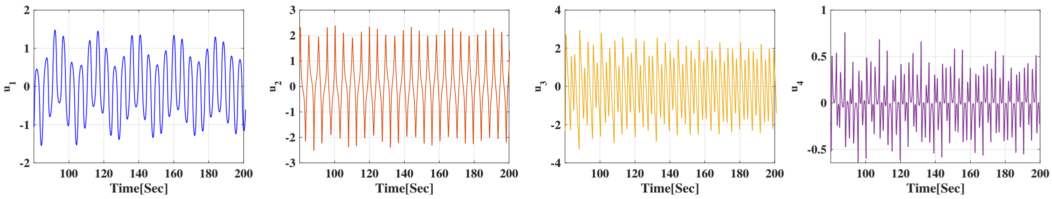

Figure 19. Time-series evolution of the states for Case 2 at $t = 200$.

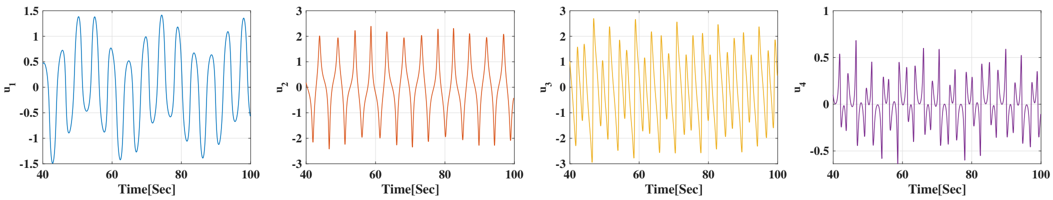

Figure 20. Time-series evolution of the states for Case 3 at $t = 100$.

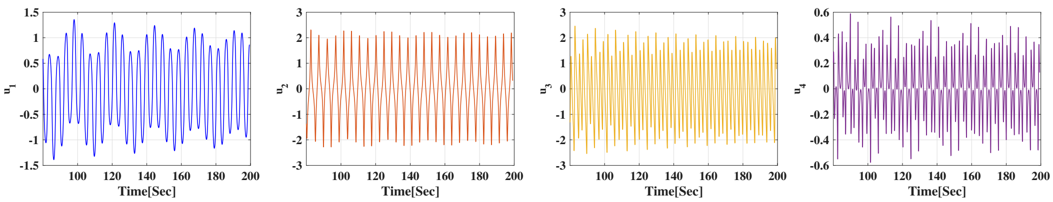

Figure 21. Time-series evolution of the states for Case 3 at $t = 200$.

5. Numerical Solutions

In this section, we investigate the influence of different variable-order functions on the numerical behavior of the proposed fractional system. Tables 6–8 present the numerical solutions of the proposed variable-order fractional system for the three considered cases. In all cases, the state variable u_1 increases monotonically from 0.2 to approximately 0.358, whereas u_2 gradually decreases from 0.3 to about 0.047. The variable u_3 changes its positive value to almost −1.63, whereas u_4 quickly falls down to achieve a steady value that is slightly negative. Despite the fact that the three variable-order functions yield highly similar trajectories, it becomes apparent that there are slight variations as time passes, signifying the importance of the order evolution in affecting the transient behavior of the system.

Table 6. Numerical solution of the proposed variable-order fractional model for Case 1.

Time	u_1	u_2	u_3	u_4
0.0	0.200000	0.300000	0.200000	0.500000
0.1	0.226421	0.258370	0.008766	0.298951
0.2	0.250989	0.224669	−0.191748	0.170166
0.3	0.272202	0.198087	−0.385395	0.094724
0.4	0.290781	0.175541	−0.573947	0.049468
0.5	0.307106	0.155178	−0.758317	0.021794
0.6	0.321375	0.135746	−0.939004	0.004679
0.7	0.333655	0.116273	−1.116256	−0.005812
0.8	0.343914	0.095880	−1.290128	−0.011859
0.9	0.352024	0.073656	−1.460505	−0.014608
1.0	0.357758	0.048549	−1.627102	−0.014560

Table 7. Numerical solution of the proposed variable-order fractional model for Case 2.

Time	u_1	u_2	u_3	u_4
0.0	0.200000	0.300000	0.200000	0.500000
0.1	0.225794	0.259259	0.013685	0.302639
0.2	0.250247	0.225550	−0.184947	0.172537
0.3	0.271525	0.198783	−0.378054	0.095483
0.4	0.290243	0.176034	−0.566831	0.049117
0.5	0.306739	0.155480	−0.751908	0.020824
0.6	0.321188	0.135867	−0.933616	0.003432
0.7	0.333643	0.116215	−1.112083	−0.007133
0.8	0.344061	0.095635	−1.287281	−0.013139
0.9	0.352309	0.073202	−1.459031	−0.015786
1.0	0.358149	0.047847	−1.626999	−0.015599

Table 8. Numerical solution of the proposed variable-order fractional model for Case 3.

Time	u_1	u_2	u_3	u_4
0.0	0.200000	0.300000	0.200000	0.500000
0.1	0.225832	0.259205	0.013395	0.302410
0.2	0.250347	0.225425	−0.185834	0.172156
0.3	0.271682	0.198602	−0.379643	0.095135
0.4	0.290441	0.175806	−0.569131	0.048890
0.5	0.306958	0.155207	−0.754872	0.020733
0.6	0.321402	0.135545	−0.937158	0.003459
0.7	0.333826	0.115828	−1.116089	−0.007010
0.8	0.344184	0.095160	−1.291613	−0.012939
0.9	0.352336	0.072601	−1.463535	−0.015513
1.0	0.358040	0.047063	−1.631500	−0.015248

For complete reproducibility, the time-varying fractional order $\alpha(t)$ is calculated explicitly for each time step t_n, and the resulting value is directly used to compute the predictor–corrector coefficients, which means that the historical memory will be updated automatically according to the order function.

The comparative study between the short-time numerical results and the long-time phase portraits demonstrates an intriguing dynamic property: even though the trajectories associated with the three different variable order functions are relatively similar within the first few integration intervals, they eventually separate and form different geometric attractor shapes in the asymptotic limit. This occurs due to the nonlinear nature and memory dependence that characterize fractional differential operators. The small deviations of the past memory function accumulate with time and lead to the separation of the trajectories in the asymptotic limit, forming different geometric attractors.

6. Conclusions

The present paper examines the dynamics and main features of a new 4D chaotic system modeled by means of the Liouville–Caputo VOF derivative. With the help of replacing a fixed-order fractional derivative by a variable-order one, the new model takes into account memory effects that depend on time. In order to analyze the system behavior, a numerical method using the VOF derivatives is used for solving it under three different variable-order functions. Further, a qualitative analysis of the dynamical behavior is carried out using phase portraits, time series, Lyapunov exponents spectrum, and the Kaplan–Yorke fractal dimension. Numerical simulations show the presence of chaos in the system since there exists at least one positive largest Lyapunov exponent for various values of variable-order functions. In addition, the Kaplan–Yorke dimension and phase portraits indicate that the new model has a large geometrical complexity, which allows us to obtain several chaotic attractors with different topologies. Thus, the results indicate that variable-order memory has a strong influence on the nonlinear dynamics of the system, and the Liouville–Caputo variable-order approach can be used as a powerful mathematical instrument for modeling chaotic processes, especially for engineering systems. Potential applications include chaos-based secure communication, image encryption, and pseudo-random number generation.

Author Contributions: Methodology, M.E., N.E.T. and M.A.A.; software, M.E. and M.A.A.; formal analysis, N.E.T. and W.H.; investigation, W.H.; resources, H.M.B.; writing—original draft preparation, M.E., W.H. and H.M.B.; writing—review and editing, M.E. and H.M.B. All authors have read and agreed to the published version of the manuscript.

Funding: Funding: This research was financially supported by the Deanship of Graduate Studies and Scientific Research at Qassim University (QU-APC-2026).

Data Availability Statement: The original contributions in this study are included in the article.

Acknowledgments: The researchers would like to thank the Deanship of Graduate Studies and Scientific Research at Qassim University (https://www.qu.edu.sa) for their financial support (QU-APC-2026).

Conflicts of Interest: The authors declare no conflicts of interest.

References

1. Dilmi, M.; Benallia, M. A NEW GENERAL CONFORMABLE FRACTIONAL DERIVATIVE AND SOME APPLICATIONS. *J. Fract. Calc. Appl.* **2025**, *16*, 1–16. https://doi.org/10.21608/jfca.2025.402920.1179.
2. Kaslik, E.; Sivasundaram, S. Non-existence of periodic solutions in fractional-order dynamical systems and a remarkable difference between integer and fractional-order derivatives of periodic functions. *Nonlinear Anal. Real World Appl.* **2012**, *13*, 1489–1497. https://doi.org/10.1016/j.nonrwa.2011.11.013.
3. Birs, I.; Muresan, C.I.; Both, R.; Nascu, I. A real life implementation of fractional order event based PI control. In *Proceedings of the 2020 IEEE International Conference on Automation, Quality and Testing, Robotics (AQTR)*; IEEE: New York, NY, USA, 2020; pp. 1–6. https://doi.org/10.1109/aqtr49680.2020.9129933.

4. Beenish.; Asim, M.; Boulaaras, S.; Rahman, M.U. Dynamical behaviour and solutions in the fractional Gross–Pitaevskii model. *Math. Comput. Model. Dyn. Syst.* **2025**, *31*, 2529190. https://doi.org/10.1080/13873954.2025.2529190.
5. Jain, S.; Sharma, A.; Bharti, A.; Singh, R., Biological application of fractal-fractional calculus. In *Recent Developments in Theory and Applications of Fractional Order Systems*; Elsevier: Amsterdam, The Netherlands, 2026; pp. 261–286. https://doi.org/10.1016/b978-0-44-323952-6.00023-7.
6. Garrappa, R.; Giusti, A.; Mainardi, F. Variable-Order Fractional Calculus: from Old to New Approaches. In *Proceedings of the 2023 International Conference on Fractional Differentiation and Its Applications (ICFDA)*; IEEE: New York, NY, USA, 2023; pp. 1–6. https://doi.org/10.1109/icfda58234.2023.10153379.
7. Luchko, Y. A New Fractional Calculus Model for the Two-dimensional Anomalous Diffusion and its Analysis. *Math. Model. Nat. Phenom.* **2016**, *11*, 1–17. https://doi.org/10.1051/mmnp/201611301.
8. De Keyser, R.; Mihai, M.D.; Birs, I.R.; Muresan, C.I. Straightforward Design of a Robust Fractional-Order Controller. *Fractal Fract.* **2026**, *10*, 330. https://doi.org/10.3390/fractalfract10050330.
9. Maione, G.; Punzi, A. Combining differential evolution and particle swarm optimization to tune and realize fractional-order controllers. *Math. Comput. Model. Dyn. Syst.* **2013**, *19*, 277–299. https://doi.org/10.1080/13873954.2012.745006.
10. Yang, X.J., Fractional Derivatives of Variable Order with Respect to Another Function and Applications. In *General Fractional Derivatives*; Chapman and Hall/CRC: Boca Raton, FL, USA, 2019; pp. 267–288. https://doi.org/10.1201/9780429284083-5.
11. Gunasekar, T.; Dhanasekar, J.P.; Anakira, N.; Ogilat, O.; Sheimat, A. Variable-Order Fractional Differential Equations: Existence, Stability, and Application to 3D Noise Evolution. *Stat. Optim. Inf. Comput.* **2026**, *16*, 641–659. https://doi.org/10.19139/soic-2310-5070-4095.
12. Patnaik, S.; Hollkamp, J.P.; Semperlotti, F. Applications of variable-order fractional operators: a review. *Proc. R. Soc. A Math. Phys. Eng. Sci.* **2020**, *476*, 20190498. https://doi.org/10.1098/rspa.2019.0498.
13. Coimbra, C.F. Mechanics with variable-order differential operators. *Ann. Phys.* **2003**, *515*, 692–703.
14. Sun, H.; Chen, W.; Chen, Y. Variable-order fractional differential operators in anomalous diffusion modeling. *Phys. A Stat. Mech. Appl.* **2009**, *388*, 4586–4592.
15. Salman, H.; Kader, A.A.; Kamal, F. Analysis of a novel fractional-order chaotic circuit with a feedback memristor: design, dynamics, and application. *Gulf J. Math.* **2025**, *19*, 340–368.
16. Zheng, X.; Li, Y.; Cheng, J.; Wang, H. Inverting the variable fractional order in a variable-order space-fractional diffusion equation with variable diffusivity: analysis and simulation. *J. Inverse -Ill-Posed Probl.* **2020**, *29*, 219–231. https://doi.org/10.1515/jiip-2019-0040.
17. Ngo, H.T.B.; Razzaghi, M.; Vo, T.N. Fractional-order Chelyshkov wavelet method for solving variable-order fractional differential equations and an application in variable-order fractional relaxation system. *Numer. Algorithms* **2022**, *92*, 1571–1588. https://doi.org/10.1007/s11075-022-01354-3.
18. Xue, G.; Lin, F.; Su, G. The Maximum Principle for Variable-Order Fractional Diffusion Equations and the Estimates of Higher Variable-Order Fractional Derivatives. *Front. Phys.* **2020**, *8*, 580554. https://doi.org/10.3389/fphy.2020.580554.
19. Sabermahani, S.; Ordokhani, Y.; Rahimkhani, P., Application of fractional-order Fibonacci wavelets to solve variable-order fractional partial differential equations. In *Recent Trends in Fractional Calculus and Its Applications*; Elsevier: Amsterdam, The Netherlands, 2024; pp. 53–73. https://doi.org/10.1016/b978-0-44-318505-2.00010-6.
20. Elbadri, M.; Abdoon, M.A.; Alzahrani, A.B.M.; Saadeh, R.; Berir, M. A Comparative Study and Numerical Solutions for the Fractional Modified Lorenz–Stenflo System Using Two Methods. *Axioms* **2024**, *14*, 20. https://doi.org/10.3390/axioms14010020.
21. Saadeh, R.; A. Abdoon, M.; Qazza, A.; Berir, M. A Numerical Solution of Generalized Caputo Fractional Initial Value Problems. *Fractal Fract.* **2023**, *7*, 332. https://doi.org/10.3390/fractalfract7040332.
22. Elbadri, M.; Al-kuleab, N.; Saadeh, R.; Hafez, M.; Abdoon, M.A. Dynamics and Chaos Analysis of the Fractional-Order Lü System Using a Hybrid Approach. *Fractal Fract.* **2026**, *10*, 51. https://doi.org/10.3390/fractalfract10010051.
23. Ahmed, A.I.; Elbadri, M.; Alotaibi, A.M.; Ashmaig, M.A.M.; Dafaalla, M.E.; Kadri, I. Chaos and Dynamic Behavior of the 4D Hyperchaotic Chen System via Variable-Order Fractional Derivatives. *Mathematics* **2025**, *13*, 3240. https://doi.org/10.3390/math13203240.
24. Ahmed, A.I.; Elbadri, M.; Al-kuleab, N.; AlMutairi, D.M.; Taha, N.E.; Dafaalla, M.E. Chaos and Bifurcations in the Dynamics of the Variable-Order Fractional Rössler System. *Mathematics* **2025**, *13*, 3695. https://doi.org/10.3390/math13223695.
25. Khashan, K.H.; Elgezouli, D.E.; Abdoon, M.A. Dynamics and Chaos Analysis of a Novel 4D Chaotic System Using Constant- and Variable-Order Fractional Calculus. *Mathematics* **2026**, *14*, 2537. https://doi.org/10.3390/math14142537.
26. Cheng, Z.; Zhang, W.; Li, M.; Shang, Y.; Xin, Y. Dynamic analysis of a generalized fractional-order model under a variable-order integral–derivative controller with delayed feedback. *Asian J. Control* 2026, *Early View*. https://doi.org/10.1002/asjc.70149.
27. Zhao, X.; Sun, Z.z.; Karniadakis, G.E. Second-order approximations for variable order fractional derivatives: Algorithms and applications. *J. Comput. Phys.* **2015**, *293*, 184–200. https://doi.org/10.1016/j.jcp.2014.08.015.

28. Clemente-López, D.; Munoz-Pacheco, J.M.; de Jesus Rangel-Magdaleno, J.; Vargas-Cabrera, L. Unified scientific tool to investigate fractional derivatives of arbitrary variable order with time-memory and order-memory: The VOFD Python package. *AIMS Math.* **2026**, *11*, 5798.
29. Zaamoune, F.; Zerimeche, H.; Ibrahim, R.; Karimov, A. Scalable Fixed-Time Synchronization of Robotic Swarms via a Novel 4D Fractional-Order System without Equilibrium Points and with Bistable Dynamics. *Izv. VUZ Appl. Nonlinear Dyn.* **2026**, *34*, 349–370. https://doi.org/10.18500/0869-6632-003219.
30. Oldham, K.B.; Spanier, J. *The Fractional Calculus: Theory and Applications of Differentiation and Integration to Arbitrary Order*; Elsevier: Amsterdam, The Netherlands, 1974; Volume 111.
31. Alqahtani, A.M.; Chaudhary, A.; Dubey, R.S.; Sharma, S. Comparative Analysis of the Chaotic Behavior of a Five-Dimensional Fractional Hyperchaotic System with Constant and Variable Order. *Fractal Fract.* **2024**, *8*, 421. https://doi.org/10.3390/fractalfract8070421.
32. Butt, A.; Ahmad, W.; Rafiq, M.; Baleanu, D. Numerical analysis of Atangana-Baleanu fractional model to understand the propagation of a novel corona virus pandemic. *Alex. Eng. J.* **2022**, *61*, 7007–7027.
33. Solís-Pérez, J.; Gómez-Aguilar, J.; Atangana, A. Novel numerical method for solving variable-order fractional differential equations with power, exponential and Mittag-Leffler laws. *Chaos Solitons Fractals* **2018**, *114*, 175–185. https://doi.org/10.1016/j.chaos.2018.06.032.
34. Mees, A.; Sparrow, C. Some tools for analyzing chaos. *Proc. IEEE* **1987**, *75*, 1058–1070. https://doi.org/10.1109/proc.1987.13849.
35. Özer, A.; Akın, E. Tools for detecting chaos. *Sak. Univ. J. Sci.* **2005**, *9*, 60–66.
36. Tian, H.; Yi, X.; Zhang, Y.; Wang, Z.; Xi, X.; Liu, J. Dynamical Analysis, Feedback Control Circuit Implementation, and Fixed-Time Sliding Mode Synchronization of a Novel 4D Chaotic System. *Symmetry* **2025**, *17*, 1252. https://doi.org/10.3390/sym17081252.
37. Sahin, M.E.; Cam Taskiran, Z.G.; Guler, H.; Hamamci, S.E. Application and Modeling of a Novel 4D Memristive Chaotic System for Communication Systems. *Circuits Syst. Signal Process.* **2020**, *39*, 3320–3349. https://doi.org/10.1007/s00034-019-01332-6.
38. El-Sayed, A.; Nour, H.; Elsaid, A.; Matouk, A.; Elsonbaty, A. Circuit realization, bifurcations, chaos and hyperchaos in a new 4D system. *Appl. Math. Comput.* **2014**, *239*, 333–345. https://doi.org/10.1016/j.amc.2014.04.109.
39. Ma, J.; Yang, Y. Hyperchaos Numerical Simulation and Control in a 4D Hyperchaotic System. *Discret. Dyn. Nat. Soc.* **2013**, *2013*, 980578. https://doi.org/10.1155/2013/980578.
40. Madani, Y.A.; Aldwoah, K.; Younis, B.; Alsharafi, M.; Osman, O.; Muflh, B. Analysis and secure communication applications of a 4D chaotic system with transcendental nonlinearities. *Sci. Rep.* **2025**, *15*, 14104. https://doi.org/10.1038/s41598-025-98807-1.